Characterizing Observed Limit Cycles in the Cassini Main Engine Thrust Vector Control System

Farheen Rizvi & Raquel Weitl

Cassini Attitude Control

Jet Propulsion Laboratory, California Institute of Technology

Outline

- Cassini mission overview
- Observed stable limit cycle in long burn execution
- Possible causes for stable limit cycle
  - Unmodeled system nonlinearities
- Describing function approach
  - Explain observed limit cycle behavior
- Reproduce limit cycle analytically and through simulation
- Limit cycle characteristics comparison
  - Telemetry, analytical and simulation
- Nonlinear element input and output response
- Conclusion and recommendations

Cassini Mission Overview

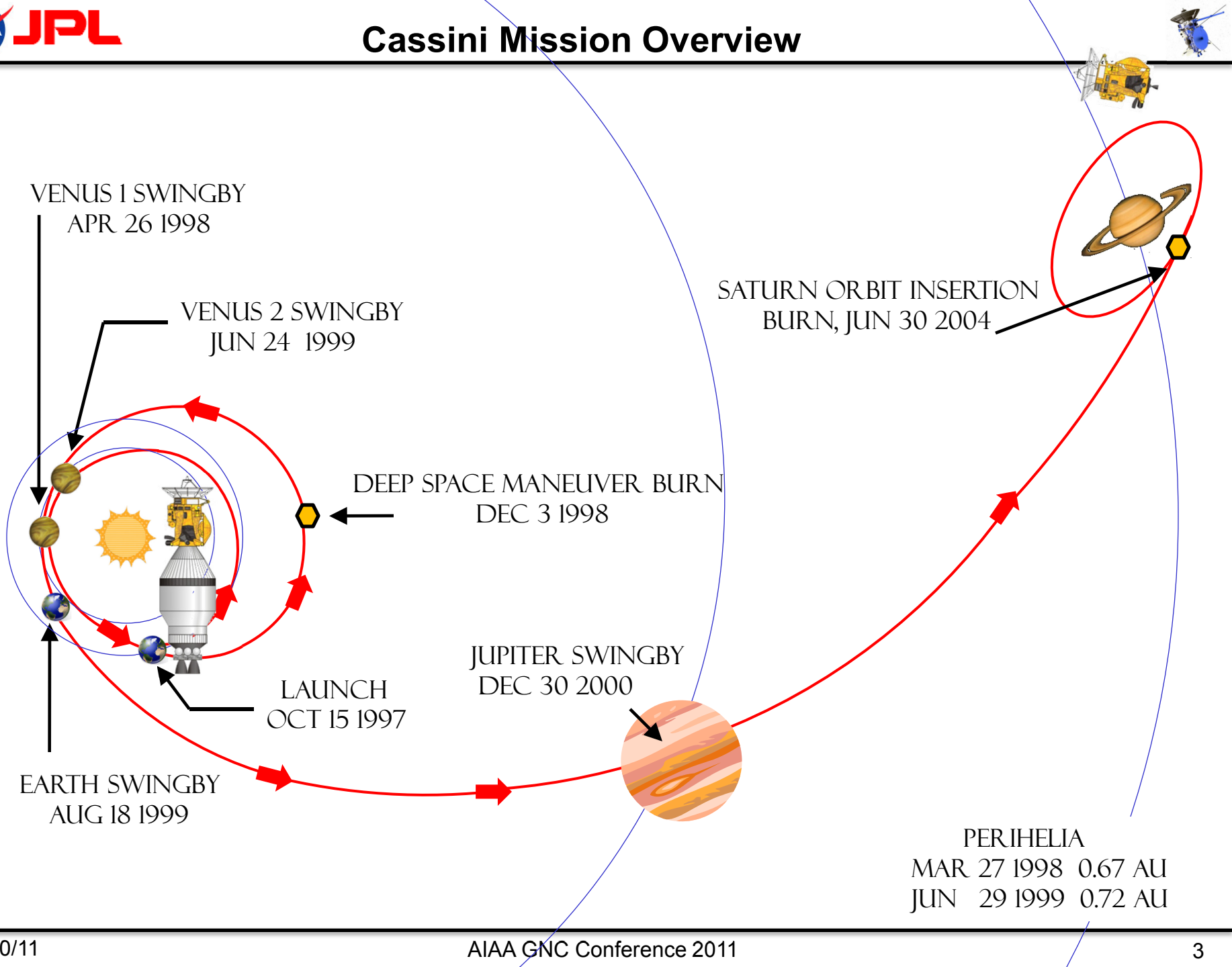

Long Burns

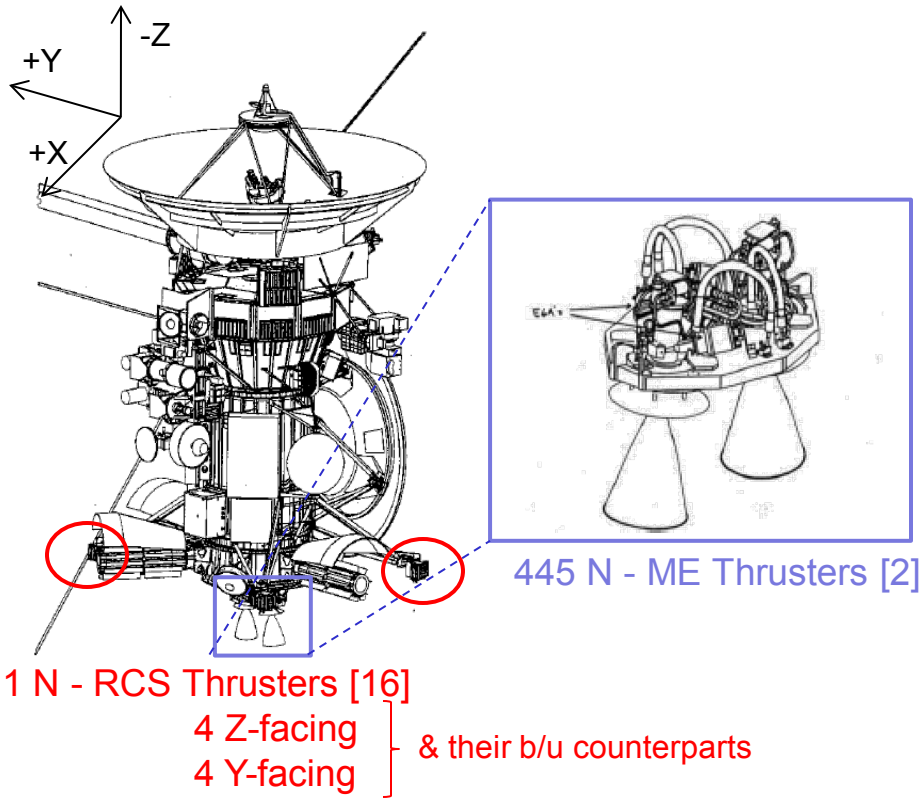

	Maneuver	Burn Time (min)
Deep Space Burns	DSM	87.6
	SOI	96.6
ME Burns	OTM 2	50
	OTM 10	2.5
	OTM 33	3.3
	OTM 144	4.2

Main Engine (ME) Orbit Trim Maneuver (OTM)
- Correction maneuvers
- Stay near a trajectory that maximizes interesting science and minimizes fuel usage
- ME OTMs only use 1 Main Engine

Long burns > 2 min

Observed Limit Cycle in Dynamics Telemetry after Long Burns

- Limit cycles observed in dynamics related telemetry (attitude, rate, errors) for long burns
- SOI burn
  - Burn duration of 96.6 min.
  - S/C X-axis rate telemetry and fast Fourier transform
  - Stable limit cycle frequency of 0.035 Hz, peak-to-peak amplitude of 1.3 x 10^{-4} rad/s

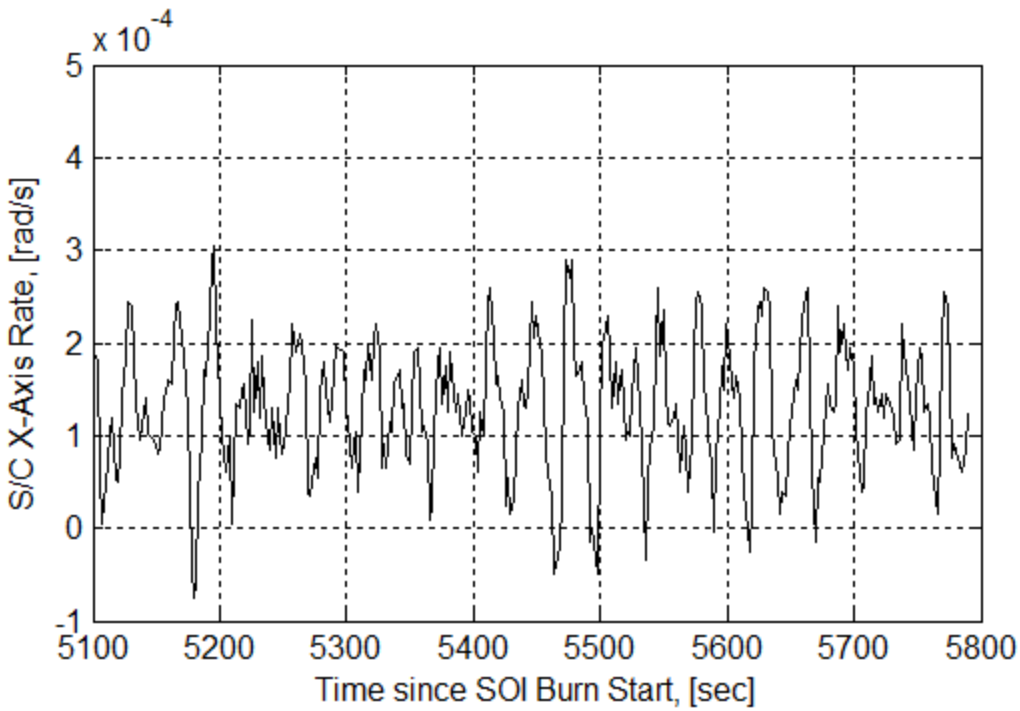

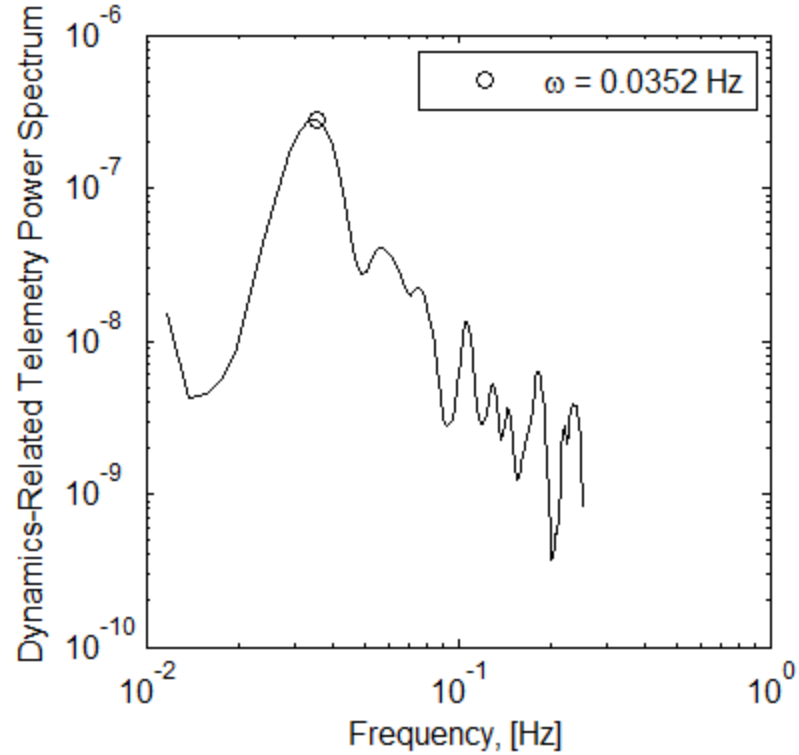

Observed Limit Cycle in Dynamics Telemetry after Long Burns

- Long ME OTM 2

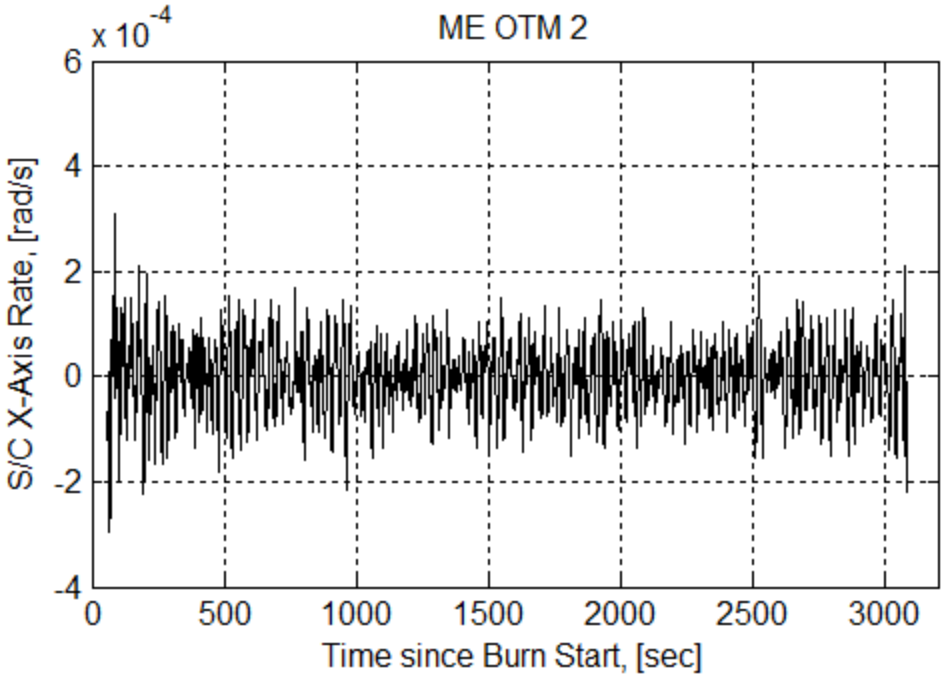

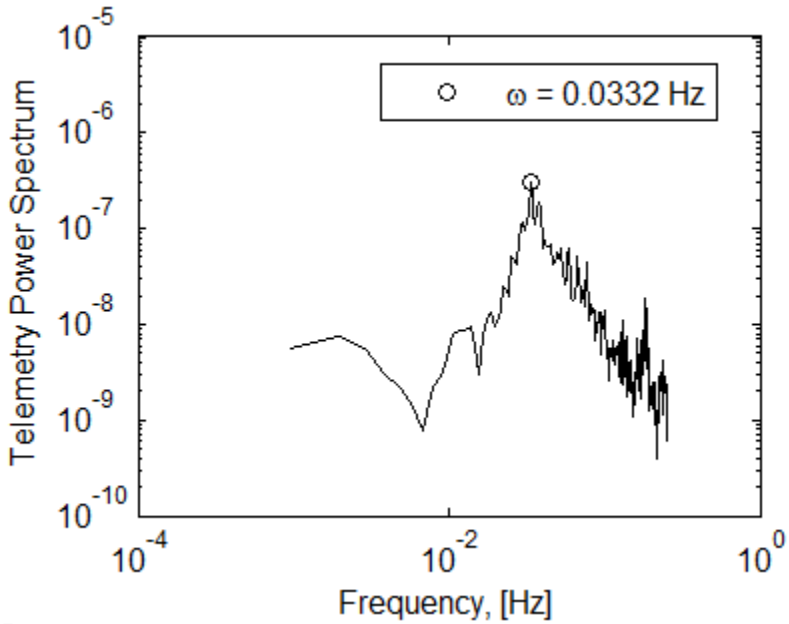

  - Burn duration of 50 min.
  - Stable limit cycle frequency of 0.033 Hz
  - Long ME OTMs: 10, 33, 144
    - Duration: 2.5 to 5 min.
    - Limit cycle frequency: 0.03 -0.05 Hz
- Limit cycles persist for extended periods during long burns
  - Dismissed that limit cycles emerge from bi-propellant sloshing motions (oscillating frequency 0.05-0.14 Hz)
    - Limit cycles dampens out on the order of minutes

Unpredicted Limit Cycle Behavior

- Main Engine Thrust Vector Control system* maintains S/C dynamics during long burns
- Performance of ME TVC system

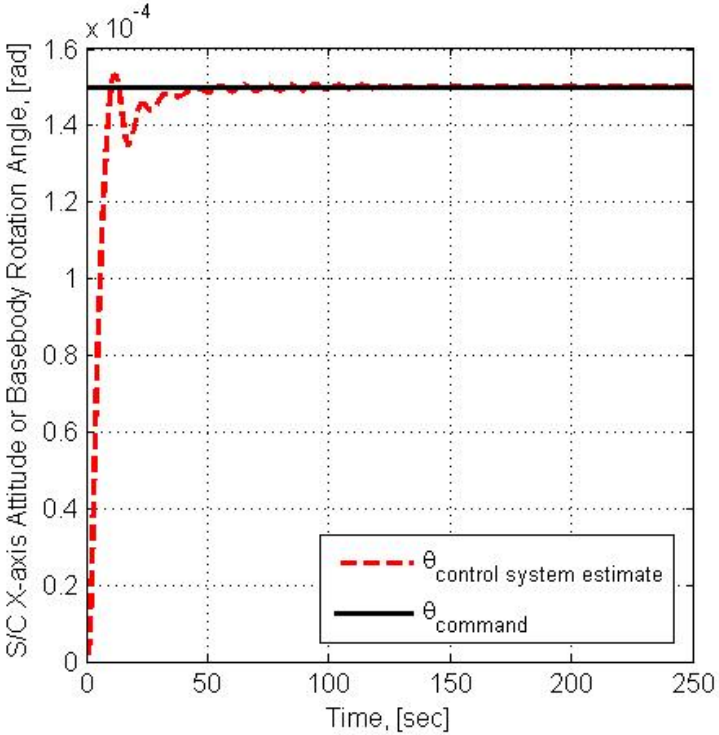

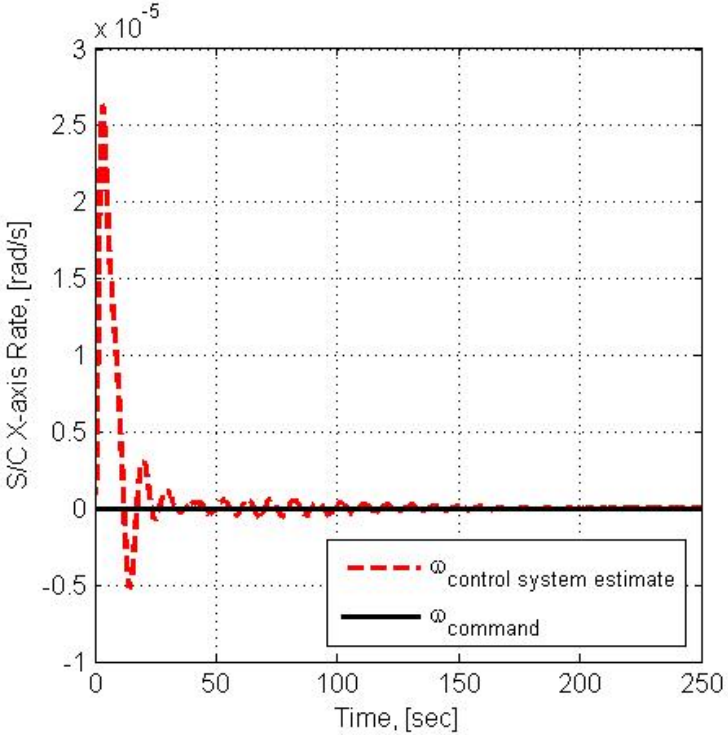

*simplified model

- Does not predict limit cycle
- In this paper, we want to study the limit cycle behavior
  - Limit cycle presence has not hindered performance to any degree of concern, however…
  - Important to understand these stable limit cycles from controller design viewpoint

Cause for Limit Cycle Occurrence

- Linear ME Thrust Vector Control system does not model system nonlinearities
- Unmodeled nonlinearities
  - propellant flex lines resistance
  - friction
  - backlash in gears
- Observed limit cycles may emerge from stable interaction between linear ME Thrust Vector Control system and unmodeled nonlinear elements*

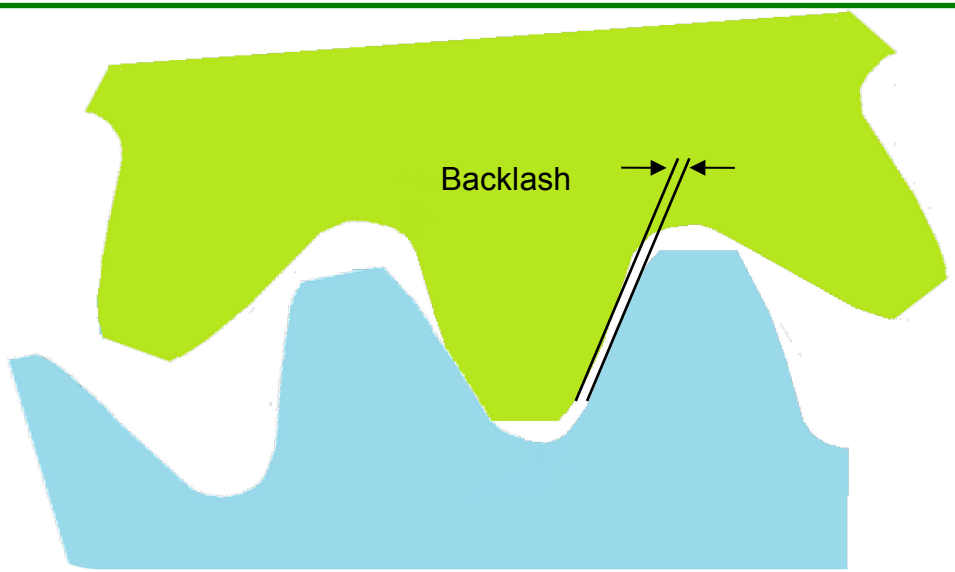

Angular Gear Clearance between mated gear teeth

- Model nonlinearity and study interaction with ME TVC system to support this idea

*Lee, A. Y., and Hanover, G., "Cassini Spacecraft Attitude Control System Flight Performance," Proceedings of the AIAA Guidance, Navigation, and Control Conference, and Exhibit, San Francisco, California, August 15-18, 2005.

Modeling Nonlinearities: Describing Function Approach

Motivation: model system nonlinearity to support that the observed limit cycle behaviors are due to the interaction between the linear control system and the nonlinearity

- One method is to represent the nonlinearity through a *Describing Function* and study its interaction with the control system
- Complex ratio of output over input

$$N = \frac{Y}{X} \angle \phi$$

where

N = describing function

X = amplitude of input sinusoid

Y = amplitude of the fundamental harmonic component of output

ϕ = phase shift of the fundamental harmonic component of output

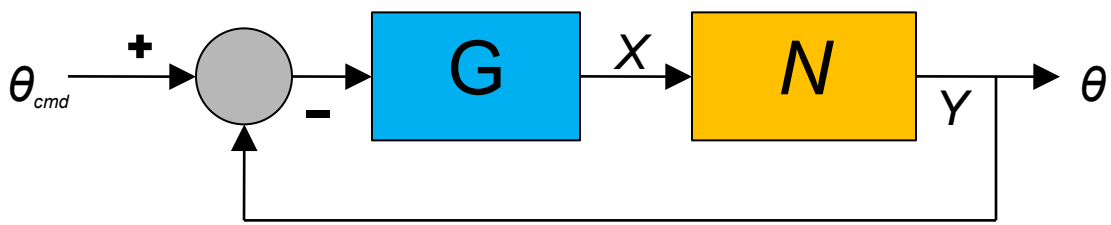

G = ME TVC system

Limit Cycle Prediction through Describing Function Analysis

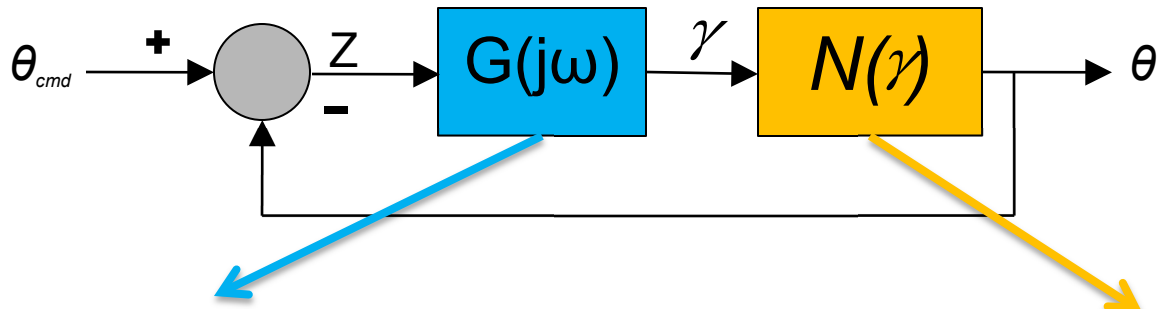

G(jω) = linear ME TVC system transfer function of input frequency, ω

N (γ)= describing function for backlash nonlinearity function of input amplitude, γ

- In order to predict limit cycle in the system, the system characteristic equation is found
- Equate elements at summation junction

$$\theta_{cmd} - \theta = Z$$

$$\theta_{cmd} - \theta = \frac{\theta}{NG} \rightarrow \theta_{cmd} = \theta + \frac{\theta}{NG} = \frac{NG \cdot \theta + \theta}{NG}$$

$$\frac{\theta}{\theta_{cmd}} = \frac{NG}{1 + NG}$$

system characteristic equation $\boxed{1 + NG = 0} \rightarrow \boxed{G(j\omega) = -\frac{1}{N(\gamma)}}$

- *limit cycle exists when relationship is satisfied*
- *oscillates at ω*
- *amplitude of γ*

Limit Cycle Characteristics

$$G(j\omega) = -\frac{1}{N(\gamma)}$$

- Examine responses for *G* and *N* for a range of ω and γ

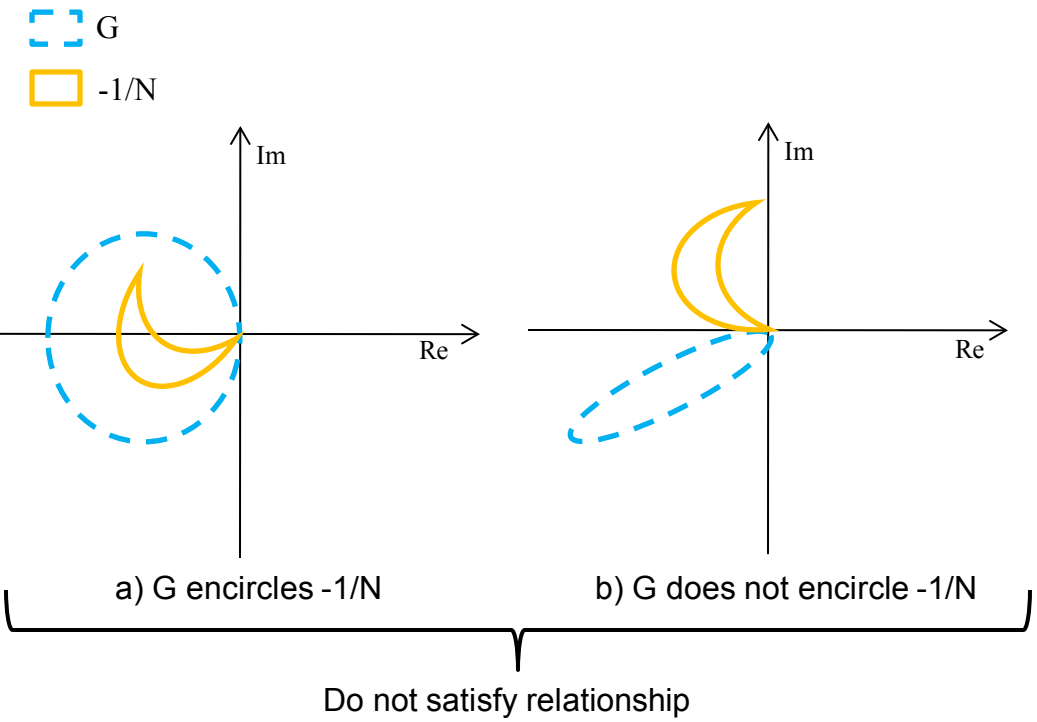

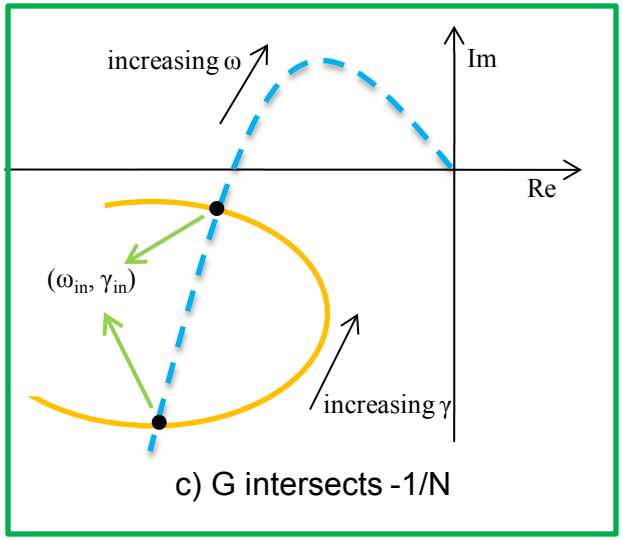

- Multiple intersection points satisfy relationship
  - Nyquist criterion determines correct intersection point
  - Criterion distinguishes between stable vs. unstable limit cycle
- Intersection point yields limit cycle characteristics
  - *G* determines oscillating frequency, ω_{in}
  - *N* determines amplitude, γ_{in}

Modeling ME TVC System and Gear Backlash

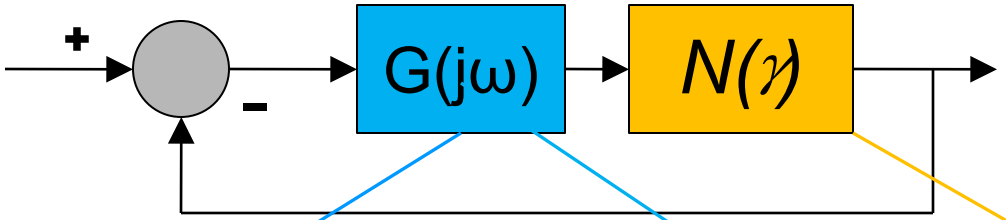

$$G(j\omega) = -\frac{1}{N(\gamma)}$$

Limit cycle characteristics

Flight Software Elements

- Controller
- Engine gimbal actuator manager

Flexible body dynamics

- magnetometer boom
- propellant slosh

Rigid body dynamics

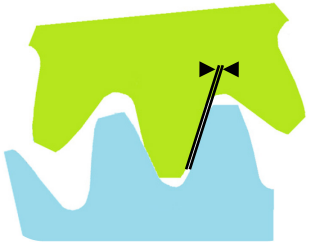

Backlash

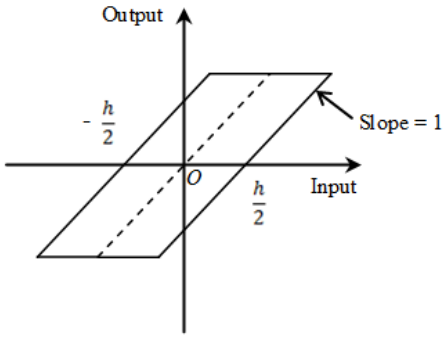

- Transfer functions for individual elements within *G*

$$G = T_{flight} T_{flex} T_{rigid}$$

- Model nonlinearity
  - Backlash element

$$\operatorname{Re} N(\gamma) = \frac{1}{\pi}\left[\frac{\pi}{2} + \arcsin(1 - h/\gamma) + 2(1 - h/\gamma)\sqrt{\frac{h}{2\gamma}\left(1 - \frac{h}{2\gamma}\right)}\right]$$

$$\operatorname{Im} N(\gamma) = \frac{2h}{\pi\gamma}\left(1 - \frac{h}{2\gamma}\right)$$

$$N(\gamma) = \operatorname{Re} N(\gamma) + \operatorname{Im} N(\gamma) j$$

h = angular gear clearance

*analyze SOI burn, model parameters are for SOI burn conditions

Analytical Limit Cycle Results (1/2)

$$G(j\omega) = -\frac{1}{N(\gamma)}$$

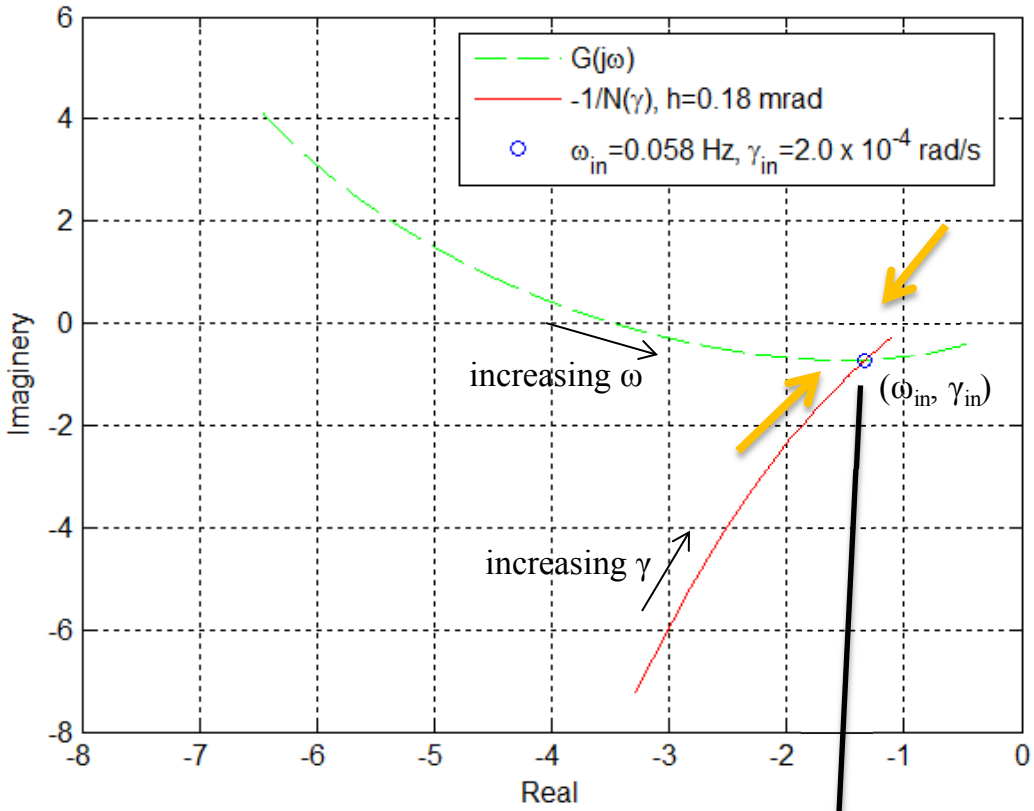

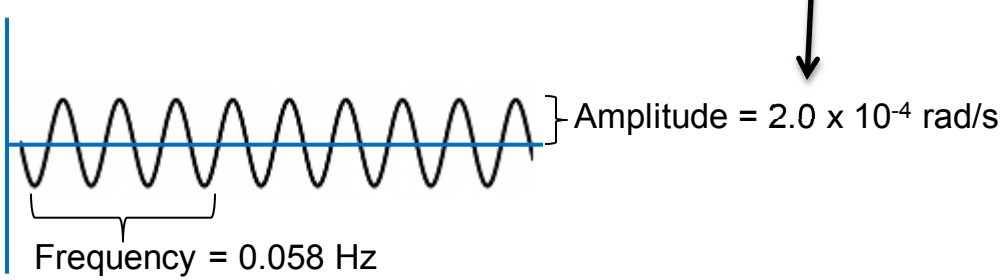

- Stable vs. unstable limit cycle
- Disturbed to left of intersection
  - From Nyquist stability criterion
    - G encircles -1/N
  - From describing function stability criterion
    - Limit cycle amplitude increases to γ_{in}
  - Converges to intersection point
- Disturbed to right of intersection
  - G does not encircle -1/N
  - Amplitude decreases to γ_{in}
  - Converges to intersection point
- Intersection point has convergent properties

- **Stable** limit cycle
  - Frequency = 0.058 Hz
  - Amplitude = 2.0 x 10^{-4} rad/s

Analytical Limit Cycle Results (2/2)

- Verify only one intersection point exists
- Examine Global response of G and -1/N

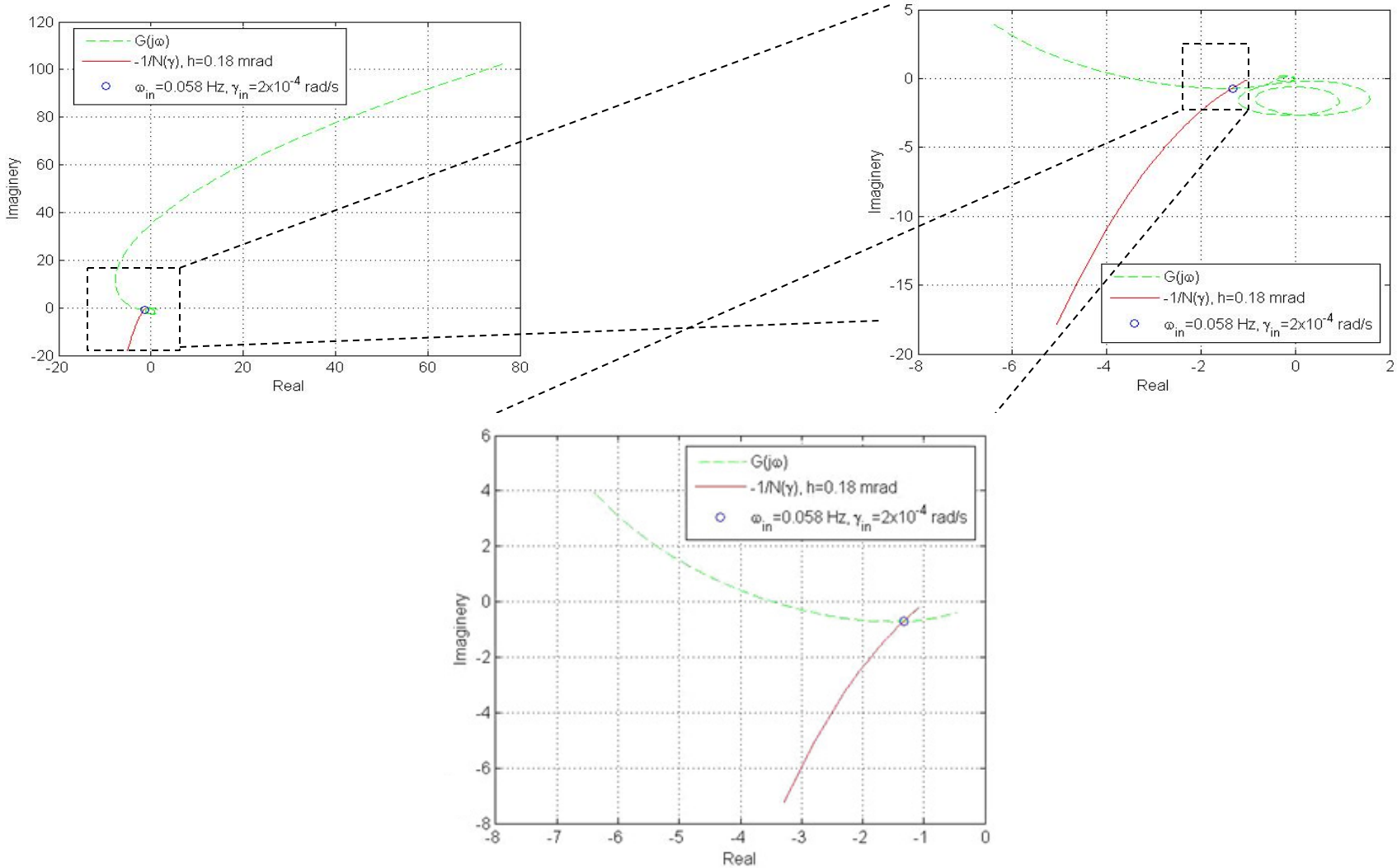

Simulation Limit Cycle Results

- Create a Simulink model for ME TVC system and nonlinearity

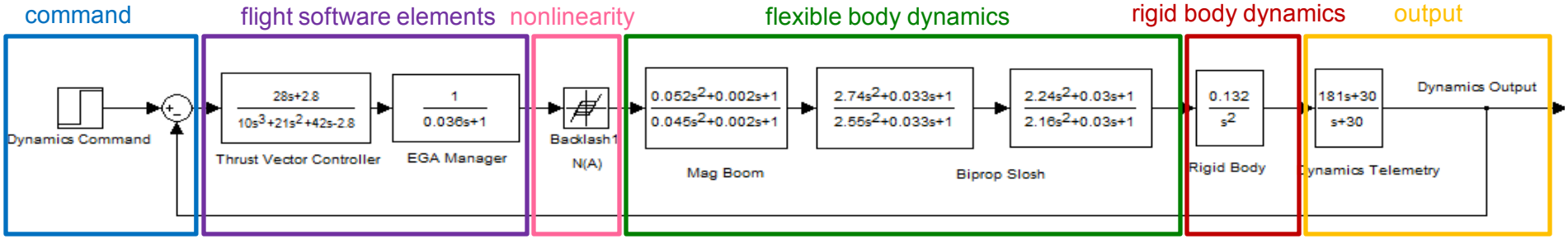

- Bi-propellant sloshing motion modeled as second-order system
  - Natural frequency = 0.1 Hz, damping ratio = 0.01, 10% settling time ≈ 6 min.

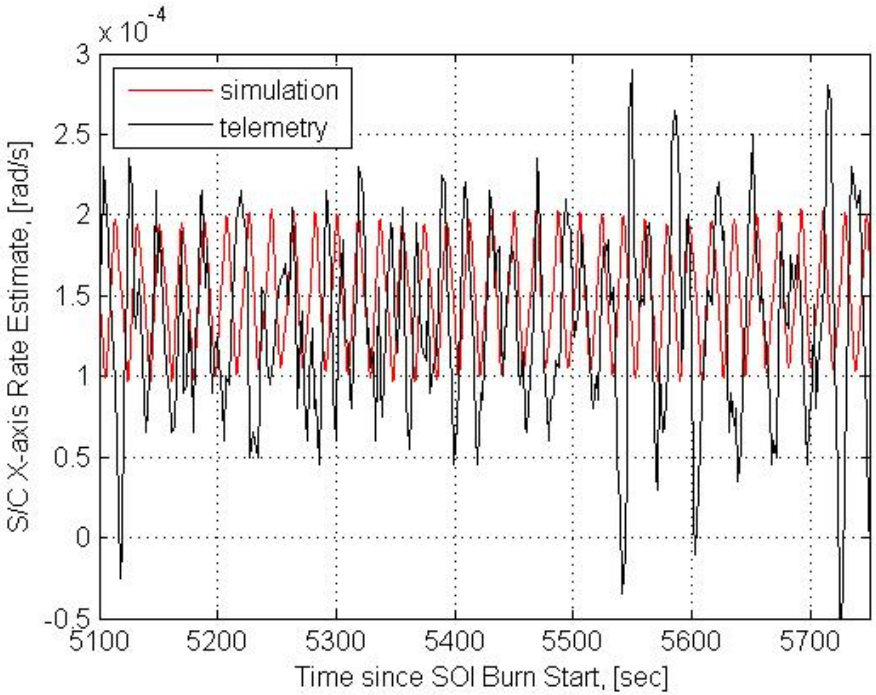

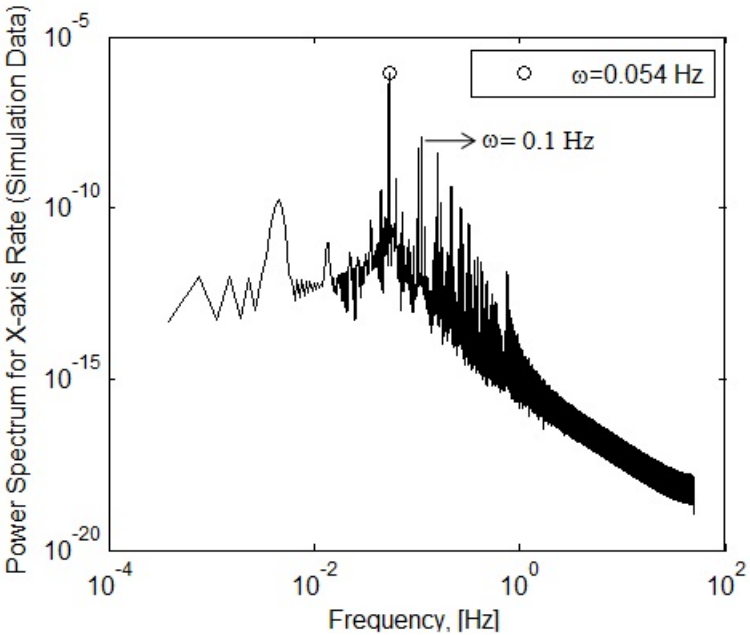

- Stable limit cycle, frequency = 0.054 Hz, amplitude = 1.0 x 10^{-4} rad/s

Backlash Nonlinearity Input and Output Characteristics

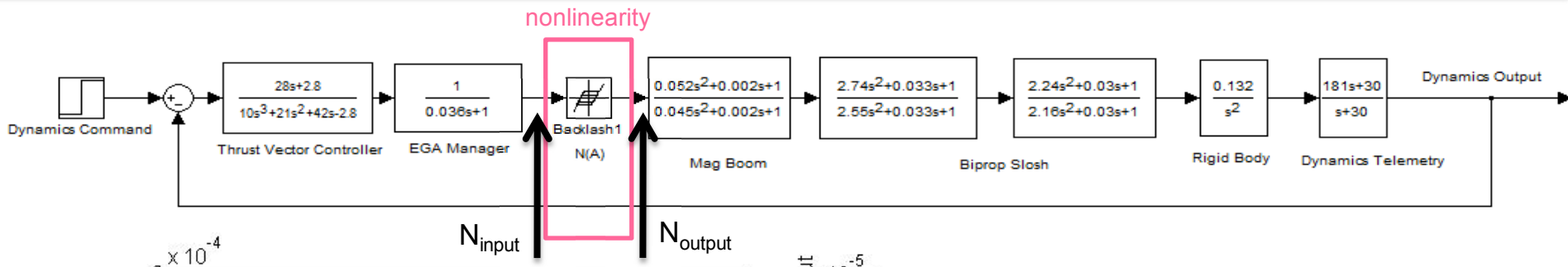

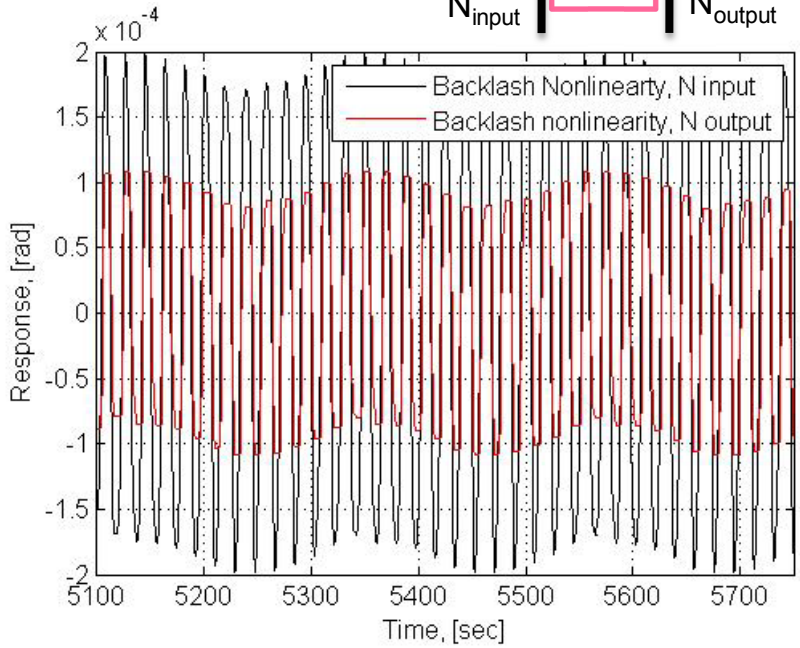

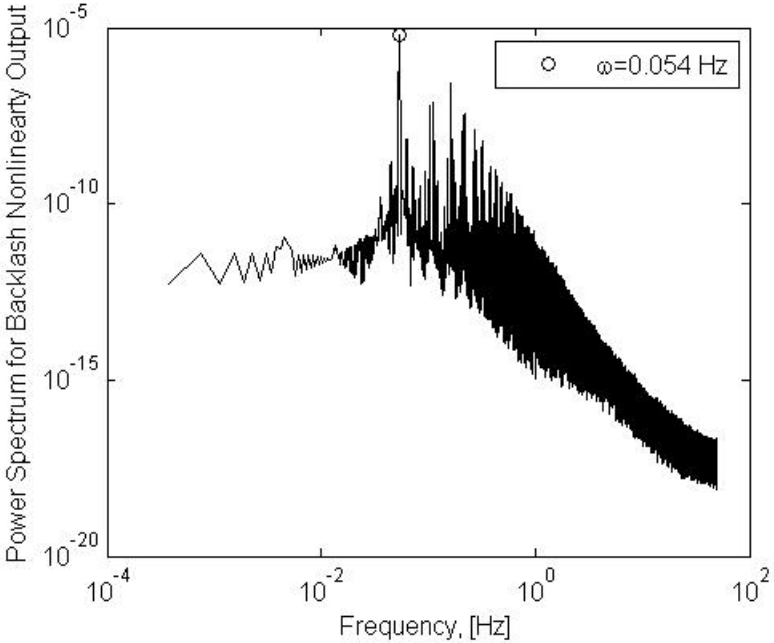

- Sinusoidal envelope for input and output
  - Inside the envelope: sinusoidal input, square wave output
- Same dominant oscillating frequency as system output
  - Frequency = 0.054 Hz
- Nonlinear element drives limit cycle
  - Without nonlinearity, a linear system does not reproduce limit cycle

Telemetry, Analytical and Simulations Results Comparison

	Limit Cycle Nature	Limit Cycle Frequency [Hz]	Limit Cycle Amplitude [rad/s]
X-axis Rate Telemetry	Stable	0.035	1.3×10^{-4}
Analytical	Stable	0.058	2.0×10^{-4}
Simulation	Stable	0.054	1.0×10^{-4}

- Agreement between telemetry data and analytical & simulation results
  - Supports that describing function theory explains observed limit cycle behavior
- Similar limit cycle characteristics
  - Same order of magnitude for frequency and amplitude
- Discrepancies
  - Simplified ME TVC system model
  - Inaccurate model parameters (exact SOI conditions)
  - Lack of representing all system nonlinearities
    - Ex. Propellant flex line resistance

Conclusions and Future Work Recommendations (1/2)

- One possible cause of the observed stable limit cycles is proposed and investigated
  - Saturn insertion burn, orbit trim maneuvers
- Limit cycles occur due to stable interaction between linear controller and unmodeled nonlinear elements
- ME TVC system performance is excellent
  - Limit cycles have not hindered performance to any degree of concern
  - Important to understand limit cycle behavior from controller design viewpoint
- Explained stable limit cycle with describing function theory
  - Create gear backlash model with describing function
  - Obtain limit cycle characteristics from interactions between gear backlash and controller responses
- Reproduced observed limit cycles in simulation (Simulink models)

Conclusions and Future Work Recommendations (2/2)

- Limit cycle has similar characteristics as observed in telemetry
  - Telemetry, analytical, and simulation results → frequency: 0.03 – 0.06 Hz, amplitude: 10^{-4} rad/s
- Discrepancies
  - Simplified ME TVC system
  - Inaccurate model parameters
  - Did not capture all system nonlinearities
- For future work:
  - Model all system nonlinearities
    - Study interaction with ME TVC system
  - More accurate model parameters
  - Nonlinear controller to capture complete system dynamics

References

- [1]Burk, Thomas, "Attitude Control Performance During Cassini Trajectory Correction Maneuvers," AIAA 2005-6270, Proceedings of the AIAA Guidance, Navigation, and Control Conference, San Francisco, California, August 15-18, 2005.

- [2]Enright, P., "Thrust Vector Control Algorithm Design for the Cassini Spacecraft," *AIAA/AHS/ASEE Aerospace Design Conference,* Irvine, California, February 16-19, 1993. AIAA paper 1993-1043.

- [3] Enright, P. and Macala, G., "Attitude and Articulation Control of the CRAF/Cassini Spacecraft In the Presence of Structural Flexibilities and Propellant Slosh", *15th Annual AAS Guidance and Control Conference,* Keystone, Colorado, February 8-12, 1992. AAS paper 92-063.

- [4]KTH Electrical Engineering Department. "Nonlinear Control Lecture 8: Compensation for back-lash and quantization". KTH Royal Institute of Technology, Stockholm, Sweden, 2006. [http://www.s3.kth.se/control/kurser/2E1262/lec08.pdf. Accessed 8/1/11.]

- [5]Lee, A. Y., and Hanover, G., "Cassini Spacecraft Attitude Control System Flight Performance," *Proceedings of the AIAA Guidance, Navigation, and Control Conference, and Exhibit*, San Francisco, California, August 15-18, 2005.

- [6]Ogata, K., *Modern Control Engineering*, Prentice Hall Inc, New Jersey, 1970, Chap.11.

- [7]Wang, Y. and Huang. Y., "Describing Function Method for Steady-State Analysis of Practical Sliding Mode Controlled Systems," Institute of Electrical Engineering, Yuan Ze University, Chungli, Taiwan, (unpublished) [http://med.ee.nd.edu/MED9/Papers/Nonlinear_control/Nonlinear_2/MED01-010.pdf. Accessed 8/1/11.]

Back-up Slides

Acknowledgements

- E.H.Kopf[1], Allan Lee[1], and Glenn Macala[1]
  - Foundation for this work
- Thomas Burk[1]
  - Historical background on SOI burn
- David Bates[1], Thomas Burk[1] , Allan Lee[1], Sima Lisman[2], and Daniel Nelson[3]
  - Peer review of this paper

[1]Cassini attitude control
[2]Guidance and control operations
[3]JPL Cabling Engineer summer intern (SMAP project)

Diagram of ME TVC System

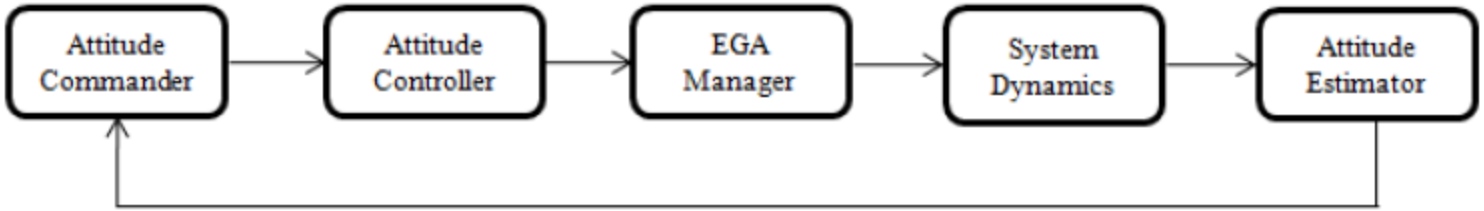

Mass Properties Comparison

Table 1: Mass Properties at Launch and SOI, and Model Mass Properties

	Launch	Pre-SOI	Post-SOI	Model
X-Axis Moment of Inertia, Ixx, [kg-m^2]	8580	8720	8040	8580
Propellant mass, [kg]	3142	2089	1240	1571
Bipropellant Fill, [%]	100	65	40	50

From Table 1, the model parameters correspond to the properties during the middle of the SOI burn. The data used in this study represents an average of the process during the entire SOI burn. Thus, the current model parameters are used as a decent average for the SOI burn.

TVC Controller Block Composition

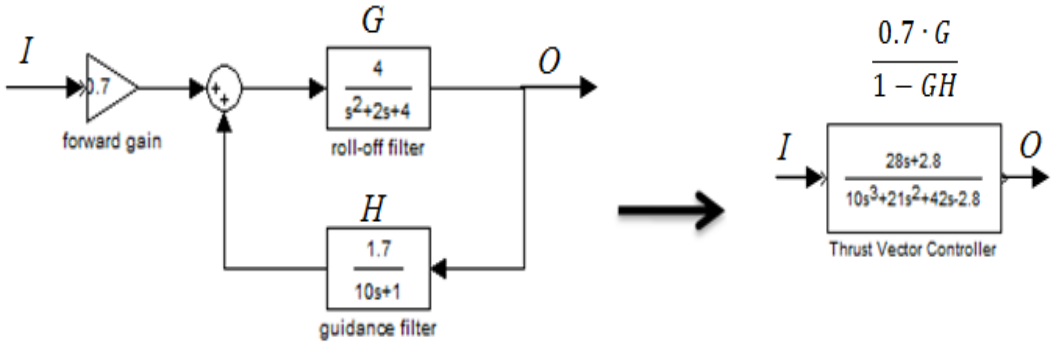

$$0.7I + HO = \frac{O}{G} \rightarrow \frac{O}{I} = \frac{0.7 \cdot G}{1 - GH} = \frac{28s + 2.8}{10s^3 + 21s^2 + 42s - 2.8}$$

Individual Transfer Functions for Elements in ME TVC System

$$T_{EGA} = \frac{1}{0.036s+1}$$

$$T_{mag} = \frac{0.052s^2+0.002s+1}{0.045s^2+0.002s+1}$$

$$T_{prop1} = \frac{A_{n1}s^2+B_{n1}s+C_{n1}}{A_{d1}s^2+B_{d1}s+C_{d1}} = \frac{2.74s^2+0.033s+1}{2.55s^2+0.033s+1}$$

$$T_{prop2} = \frac{A_{n2}s^2+B_{n2}s+C_{n2}}{A_{d2}s^2+B_{d2}s+C_{d2}} = \frac{2.24s^2+0.03s+1}{2.16s^2+0.03s+1}$$

$$T_{sc} = \frac{0.0001716s^2+0.132}{s^2} \approx \frac{0.132}{s^2} = \frac{I_{xx-m}}{s^2}$$

Bi-propellant Sloshing Transfer Functions

$$T_{prop1} = \frac{A_{n1}s^2 + B_{n1}s + C_{n1}}{A_{d1}s^2 + B_{d1}s + C_{d1}} = \frac{2.74s^2 + 0.033s + 1}{2.55s^2 + 0.033s + 1}$$

$$T_{prop2} = \frac{A_{n2}s^2 + B_{n2}s + C_{n2}}{A_{d2}s^2 + B_{d2}s + C_{d2}} = \frac{2.24s^2 + 0.03s + 1}{2.16s^2 + 0.03s + 1}$$

The bi-propellant slosh transfer functions are modeled as a second-order system with a natural frequency and damping ratio of 0.1 Hz and 0.01, respectively. These yield a 10% settling time of 6 min. for the oscillations emerging from the bi-propellant slosh modes. Thus after 6 min., the system oscillations due to bi-propellant sloshing motion diminish and the system response settles to the commanded spacecraft dynamics. This further supports that prolonged stable limit cycles do not emerge from the bi-propellant sloshing motions.

Moment of Inertia Parameter

$$T_{sc} = \frac{0.0001716s^2 + 0.132}{s^2} \approx \frac{0.132}{s^2} = \frac{I_{xx-m}}{s^2}$$

The moment of inertia parameter, can be approximated as the function of spacecraft X-axis moment of inertia, I_{xx}, thrust force, F, and lever arm, L.

$$I_{xx-m} = \frac{FL}{I_{xx}}$$

The main engine outputs 445 N of thrust and is located 1.96 m from the spacecraft center of mass during the SOI burn condition. Combining these along with the model I_{xx} yields an I_{xx-m} of 0.1 from the equation, which is close to 0.132 used in the model transfer function.

Dynamics Telemetry Block

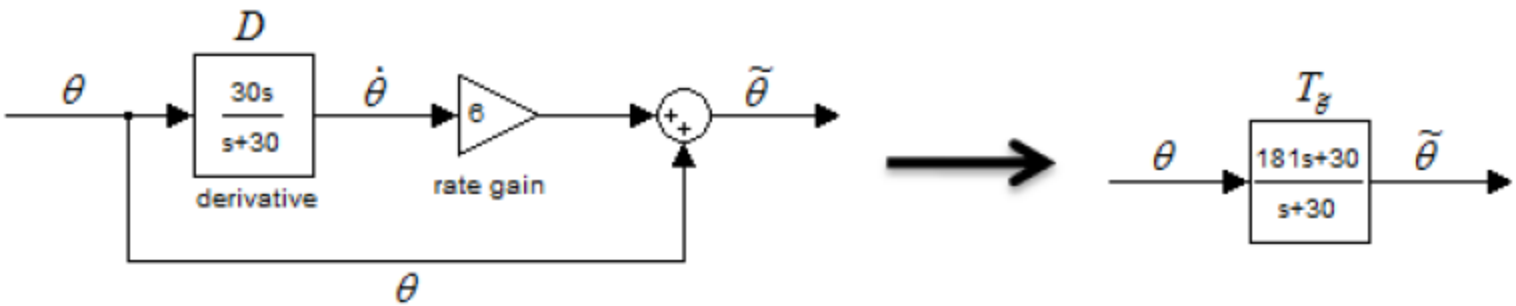

$$\theta + 6D\theta = \tilde{\theta} \rightarrow T_{\tilde{\theta}} = \frac{\tilde{\theta}}{\theta} = \frac{181s + 30}{s + 30}$$

Derivative Operator Approximation

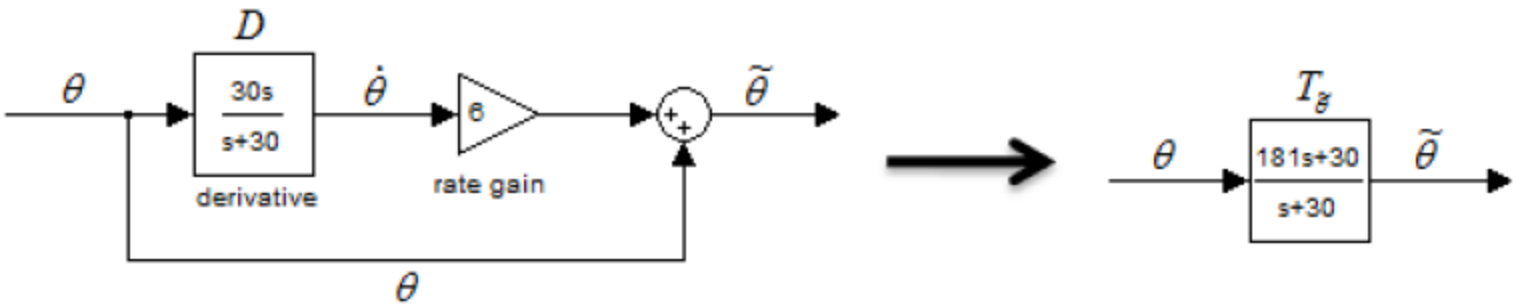

The transfer function, D, is an approximation of the derivative operator, s, which does not exist in Simulink© analysis. In this study, the frequencies of interest are ~0.03 Hz. When D is evaluated around these small frequencies, as compared with 30 Hz, the derivative operator is the result.

$$\frac{30s}{s+30} \approx \frac{\cancel{30}s}{\cancel{30}} \rightarrow s$$

$$j\omega_{small} \approx 0.03 \; to \; 0.06 \; Hz$$

Sensitivity Analysis – Bi-propellant Slosh 1 Coefficients

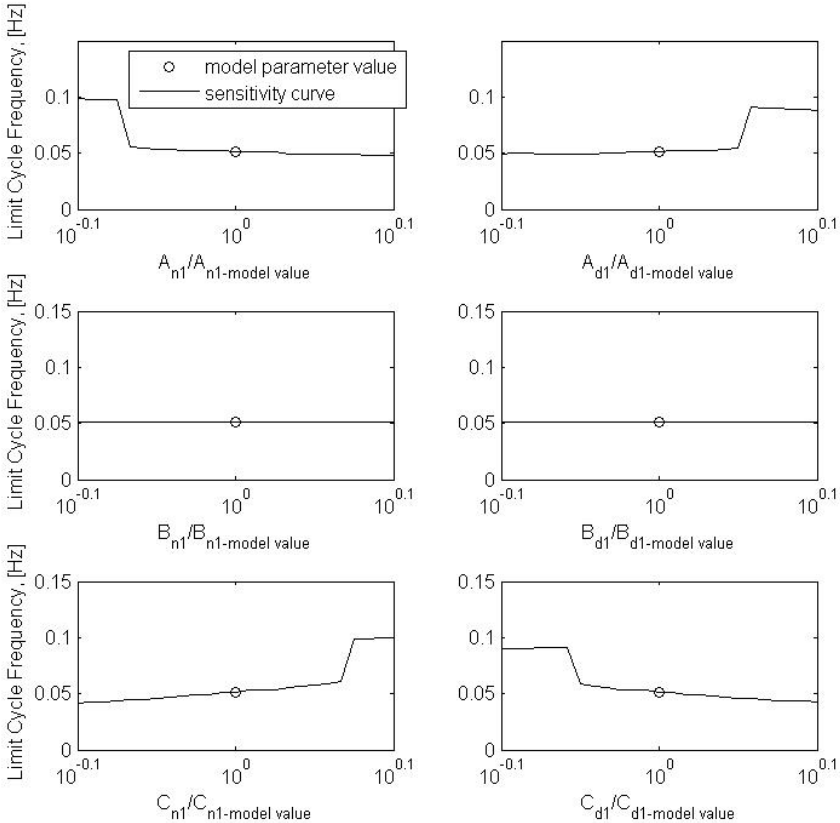

Sensitivity Analysis – Bi-propellant Slosh 2 Coefficients

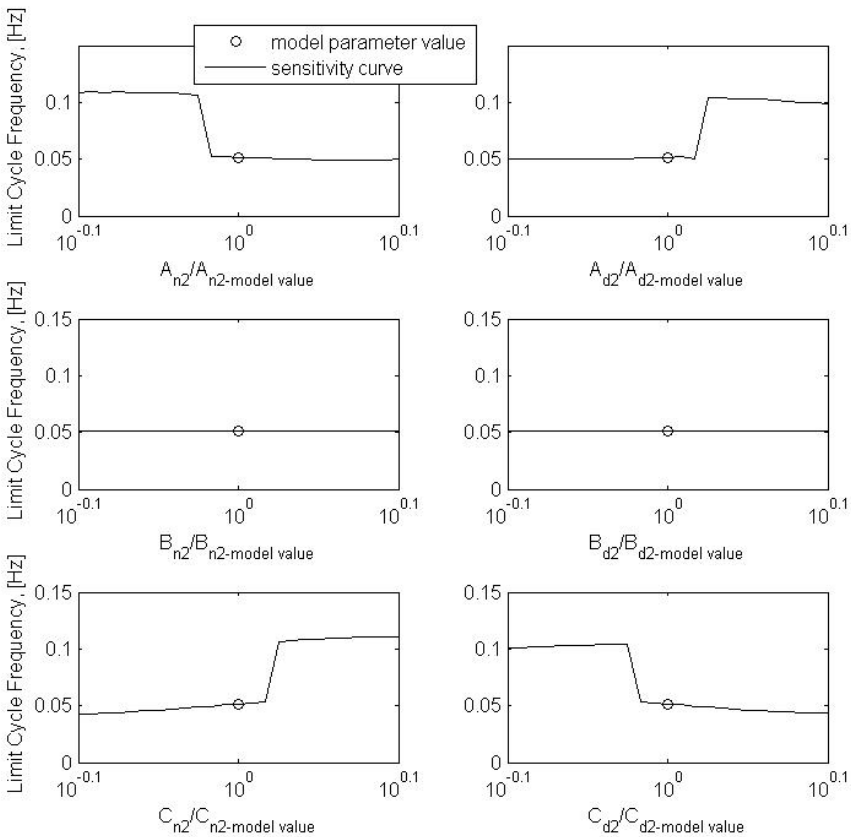

Sensitivity Analysis – Moment of Inertia and Nonlinear Parameters

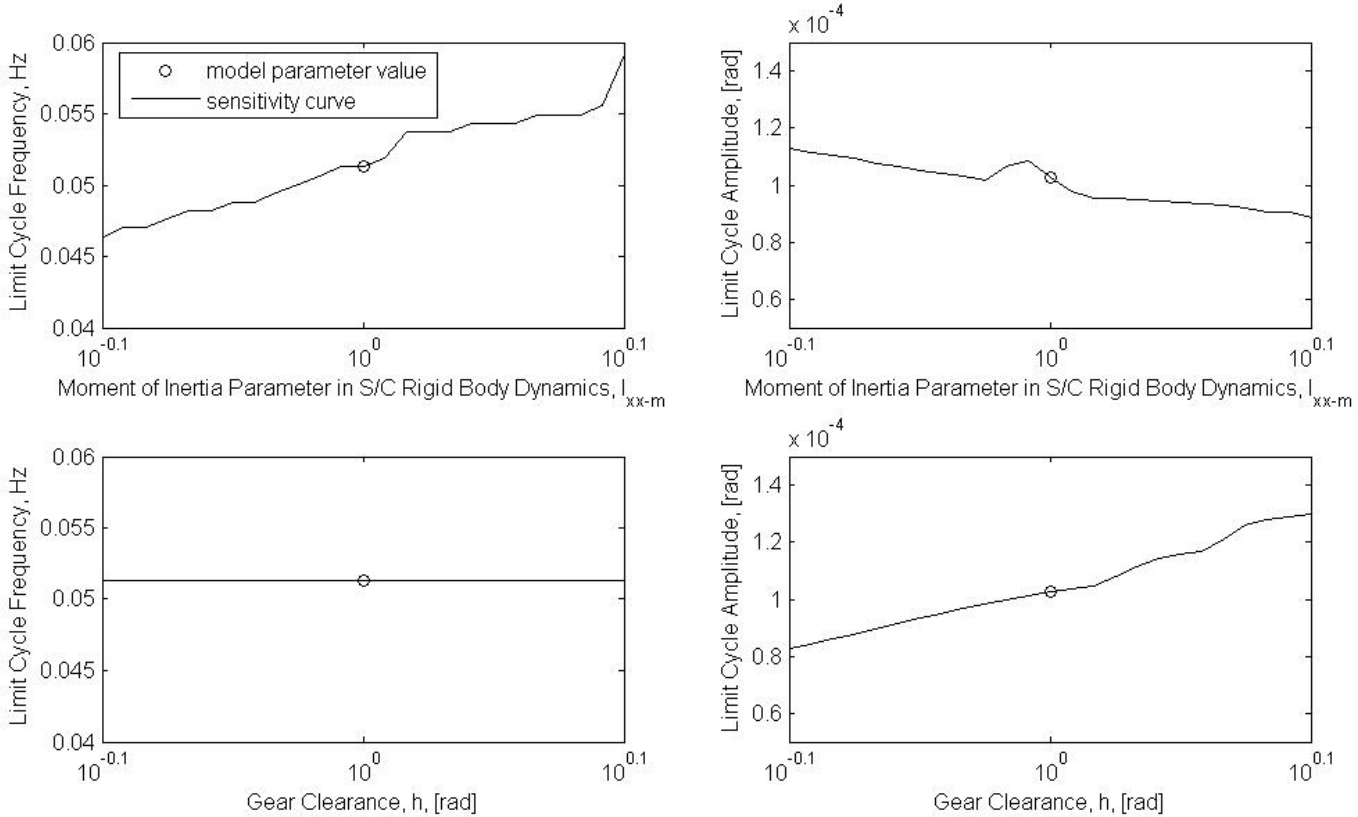
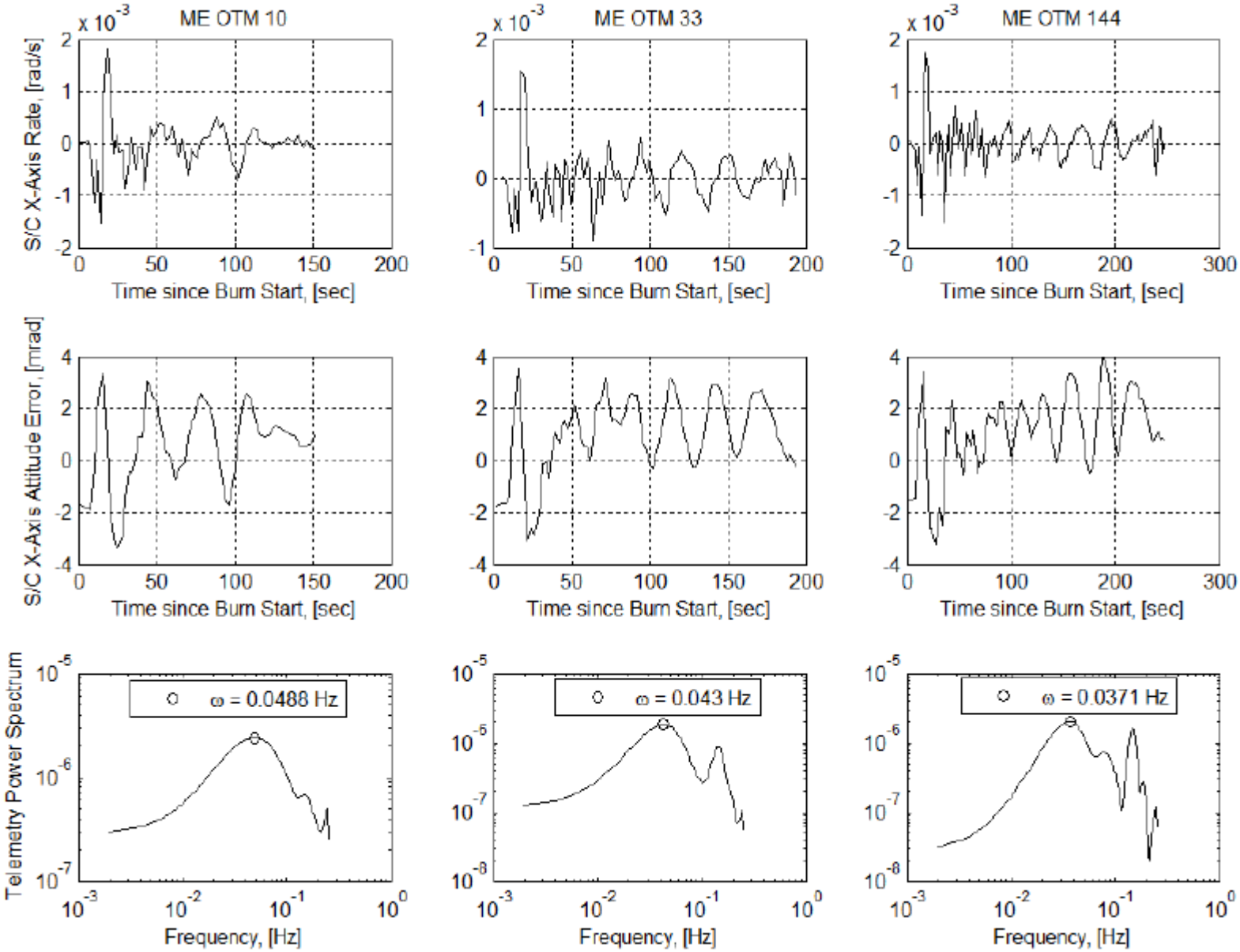
ME OTM Telemetry Data